Density Functional Theory of Lamellar Ordering in Diblock Copolymers

J. Melenkevitz and M. Muthukumar*

Polymer Science and Engineering Department, University of Massachusetts, Amherst, Massachusetts 01003

Received November 27, 1990; Revised Manuscript Received February 15, 1991

ABSTRACT: Density functional theory has been used to describe the ordering phenomena of amorphous A–B diblock copolymers. The resulting formalism was then used to study the ordering of a symmetric diblock copolymer to the lamellar morphology for values of χN above the microphase separation transition value. The number of statistical segments per diblock copolymer chain is denoted by N and χ is the Flory interaction parameter. We have identified three distinct regimes for the N dependence of the domain spacing D. For $10.495 \leq \chi N \leq 12.5$, the weak segregation limit of Leibler is realized where the domain spacing D is proportional to $N^{0.5}$. For $\chi N > 100$, the strong segregation limit is achieved where D is proportional to $N^{0.67}$. In the newly discovered intermediate regime ($15 \leq \chi N \leq 95$), D is proportional to $N^{0.72}$ and the domain boundaries support substantial fluctuations. The distinct features of the microscopic density profiles in the various regimes are discussed. In addition, the present theoretical results are compared with the most recent experimental investigations reported in the literature.

I. Introduction

Flexible noncrystalline diblock copolymers in the bulk are well-known[1-20] to form various distinct morphologies as either the temperature is lowered or the molecular weight is increased. The boundaries of the stability of the various ordered morphologies are experimentally found to depend on the composition of the diblock copolymer, the temperature, and the molecular weight of the copolymer. For diblock copolymers containing an A-type chain of degree of polymerization N_A and a B-type chain of degree of polymerization N_B, the pertinent variables are the total degree of polymerization $N = N_A + N_B$, the composition of the A-type segments $f = N_A/N$, and the temperature expressed in terms of the Flory–Huggins interaction parameter χ. For a given block copolymer composition f, as the value of χN is increased either by increasing N or by reducing the temperature, the disordered diblock copolymer melt undergoes a transition at $(\chi N)_t$ to an ordered state. For $\chi N > (\chi N)_t$, the variation of the domain spacing and the interfacial thickness of the ordered state with molecular weight and temperature has been an area of active experimental pursuit[1-20] over the past two decades.

Many theoretical investigations have been carried out to understand the phase diagram of diblock copolymers. These theories may be broadly classified into two groups. The first group, called the strong segregation theories[21-27] pioneered by Meier and Helfand, focused on the microscopic details of block copolymers in the phase-separated state at temperatures far below the microphase separation temperature appropriate for a particular morphology. The strong segregation regime is characterized by strong spatial variation of composition for the two constituents composing the diblock copolymer, along with a very narrow interface separating the domains of the two components. The total free energy of the system in the strong segregation limit is considered to consist of two contributions, one the interfacial energy and the other due to the stretching of the polymer chains that arises from the incompatibility of the two components at lower temperatures. Considering the lamellar morphology as a specific example, the competition between these two effects gives rise to the N dependence of the domain spacing D being given by

$$D \propto N^{\alpha}$$

where α is $^2/_3$ or very close to $^2/_3$.

The second class of theories[28,29] deals with the weak segregation limit. Within the weak segregation limit the microscopic density profile of the components of the diblock copolymer is considered to vary weakly and sinusoidally in space. The two chains comprising the diblock are highly interpenetrating, and the period D of the sinusoidal density profile scales as $N^{0.5}$. The first investigation into the weak segregation regime was performed by Leibler,[28] who used a Landau-type expansion in the order parameter with the vertex functions being calculated by using the random-phase approximation. Leibler then assumed that there is one dominant wave vector at which the two-body vertex function in the disordered state is a minimum in determining the free energy of the ordered state. Leibler's theory predicts a first-order transition to the body-centered cubic morphology from the disordered state for all values of f except $f = 0.5$. The parameter space where the cylindrical and lamellar morphologies become stable was also obtained. The transition at $f = 0.5$ was predicted to be continuous and the ordering is directly to the lamellar morphology. The mean field picture of Leibler was improved upon by Fredrickson and Helfand[29] by accounting for some density fluctuations in the disordered state but still assuming the dominance of one wave vector in determining the ordered state. The inclusion of the density fluctuations changes the order of the transition at $f = 0.5$ to weakly first order and suppresses the critical temperature for finite value of N while the mean field result of Leibler is recovered as $N \to \infty$. Considering the assumptions made in the weak segregation theories, they are expected to only be valid near the microphase separation transition.

Therefore there is a critical need to bridge the gap between the weak and strong segregation limits and to find conditions of validity of these limits. In view of this, we have attempted a comprehensive theory for the ordering of diblock copolymers using density functional theory. Density functional theory was first developed to study the freezing of simple liquids[30,31] and was then applied to a variety of other problems[32-38] including glass formation, surface tension of mixtures of monatomic liquids, and liquid crystals. In this paper we develop a general density functional theory for the ordering of diblock copolymers. The theory constructed is then used to describe the ordering of a symmetric diblock copolymer with lamellar morphology.

0024-9297/91/2224-4199$02.50/0

The experimental situation in determining the ranges of the weak and strong segregation limits is controversial. While most of the workers[1,18,20] claim to find the strong segregation law, $D \propto N^{2/3}$, some workers[10,19] have found a higher value of 0.8. In one recent study,[20] the exponent α had been found to be close to $^2/_3$ in agreement with the strong segregation theories, although a part of the data used in obtaining this result actually belonged to the weak segregation limit. The density functional theory of ordering of symmetric diblock copolymers to the lamellar morphology described in this paper leads to the identification of three distinct regimes:

(a) weak segregation limit

$$(\chi N_c) = 10.495 \leq \chi N \leq 12.5 \qquad D \propto N^{0.5}$$

(b) intermediate regime

$$12.5 < \chi N \leq 95 \qquad D \propto N^{0.72}$$

(c) strong segregation limit

$$100 < \chi N \qquad D \propto N^{0.67}$$

Thus we find that there exists an intermediate regime spanning almost a decade in χN, where the exponent α is higher than even in strong segregation limit. Furthermore, much of the experimental data reported in the literature actually falls in the first two regimes giving an effective exponent of around $^2/_3$, thus fortuitously implying the presence of the strong segregation limit. Our results resolve the apparent conflicting conclusions of the earlier experimental investigations.

The rest of the paper is organized as follows. The formalism of the density functional theory of diblock copolymers is presented in the next section. The calculated results and conclusions are contained in section III.

II. Formalism

Consider an A–B diblock copolymer system with chemical potential μ contained in a volume V at temperature T. Within the grand canonical description, the system is open to the number of diblock copolymer chains n. Each copolymer chain consists of N segments with the fraction of A segments in a chain being given by f. Throughout the present work we will assume that both blocks A and B have the same Kuhn statistical segment length l. Although the system considered here is a one-component system in the thermodynamic sense, there are two microscopic density variables at any space point $\mathbf{r}$, namely, $\rho_A(\mathbf{r})$ and $\rho_B(\mathbf{r})$ corresponding respectively to the local monomer densities of types A and B. Instead of describing the system in terms of $\rho_A(\mathbf{r})$ and $\rho_B(\mathbf{r})$, the total microscopic monomer density $\rho(\mathbf{r})$ and either $\rho_A(\mathbf{r})$ or $\rho_B(\mathbf{r})$ could equivalently be used since $\rho(\mathbf{r}) = \rho_A(\mathbf{r}) + \rho_B(\mathbf{r})$. Here we will use $\rho(\mathbf{r})$ and $\rho_A(\mathbf{r})$ to describe the A–B diblock copolymer system. The grand potential $\Omega[\rho_A(\mathbf{r}),\rho(\mathbf{r})]$ ($\Omega = -PV$, where P is pressure) and Helmholtz free energy $F[\rho_A(\mathbf{r}),\rho(\mathbf{r})]$ are unique functionals of the two microscopic density variables $\rho(\mathbf{r})$ and $\rho_A(\mathbf{r})$

$$\Omega[\rho(\mathbf{r}),\rho_A(\mathbf{r})] = F[\rho(\mathbf{r}),\rho_A(\mathbf{r})] - \frac{\mu}{N}\int d\mathbf{r}\, \rho(\mathbf{r}) \qquad (1)$$

Note that the chain density $\rho(\mathbf{r})/N$ is the conjugate variable to μ. The equilibrium density profiles $\rho_{A0}(\mathbf{r})$ and $\rho_0(\mathbf{r})$ for the system are determined by minimizing the grand potential functional with respect to variations in $\rho_A(\mathbf{r})$ and $\rho(\mathbf{r})$

$$\left.\frac{\delta\Omega}{\delta\rho_A(\mathbf{r})}\right|_{\rho_{A0}(\mathbf{r}),\rho_0(\mathbf{r})} = 0 \qquad \left.\frac{\delta\Omega}{\delta\rho(\mathbf{r})}\right|_{\rho_{A0}(\mathbf{r}),\rho_0(\mathbf{r})} = 0 \qquad (2)$$

Evaluated at the equilibrium densities, $\Omega[\rho_0(\mathbf{r}),\rho_{A0}(\mathbf{r})]$ and $F[\rho_0(\mathbf{r}),\rho_{A0}(\mathbf{r})]$ are the grand potential and Helmholtz free energy, respectively, for the system.

The total Helmholtz free energy functional F can conveniently be divided into two parts, an ideal contribution F_{id}, which neglects potential interactions between segments but takes into account the polymer chain connectivity, and an excess part F_{ex} due to interactions.

$$F = F_{id} + F_{ex} \qquad (3)$$

Substitution of the functional forms of $F_{id}[\rho(\mathbf{r}),\rho_A(\mathbf{r})]$ and $F_{ex}[\rho(\mathbf{r}),\rho_A(\mathbf{r})]$ into eqs 1 and 2 gives a set of two coupled self-consistent equations for the equilibrium densities $\rho_0(\mathbf{r})$ and $\rho_{A0}(\mathbf{r})$.

$$\left.\frac{\delta F_{ex}}{\delta\rho(\mathbf{r})}\right|_{\rho_{A0}(\mathbf{r}),\rho_0(\mathbf{r})} = -\left.\frac{\delta F_{id}}{\delta\rho(\mathbf{r})}\right|_{\rho_{A0}(\mathbf{r}),\rho_0(\mathbf{r})} + \frac{\mu}{N}$$

$$\left.\frac{\delta F_{ex}}{\delta\rho_A(\mathbf{r})}\right|_{\rho_{A0}(\mathbf{r}),\rho_0(\mathbf{r})} = -\left.\frac{\delta F_{id}}{\delta\rho_A(\mathbf{r})}\right|_{\rho_{A0}(\mathbf{r}),\rho_0(\mathbf{r})} \qquad (4)$$

The existence of one of the various ordered morphologies in the microphase separated state of diblock copolymers corresponds to a solution of this coupled set of equations for which $\rho_0(\mathbf{r})$ and $\rho_{A0}(\mathbf{r})$ are periodic in space. In practice, the equilibrium ordered states are found by parameterizing $\rho(\mathbf{r})$ and $\rho_A(\mathbf{r})$ with the presumed symmetries of the ordered states and minimizing Ω with respect to the variational parameters. The coexistence between the disordered phase and the ordered state occurs when T, μ, and Ω in the two phases are equal.

The key approximation of the density functional theory[30-38] of order–disorder transitions is to expand the excess Helmholtz free energy F_{ex} of the ordered state in a functional Taylor series expansion about a disordered phase with the same chemical potential μ as the ordered phase. For diblock copolymers, the homogeneous disordered phase is characterized by densities $\rho_d = \langle\rho_d(\mathbf{r})\rangle_0$ and $\rho_{Ad} = \langle\rho_{Ad}(\mathbf{r})\rangle_0$, where $\langle\ \rangle_0$ denotes the average overall density profiles in the homogeneous state. This leads to the functional expansion for $F_{ex}[\rho(\mathbf{r}),\rho_A(\mathbf{r})]$ in powers of $[\rho(\mathbf{r}) - \rho_d]$ and $[\rho_A(\mathbf{r}) - \rho_{Ad}]$ to be

$$F_{ex}[\rho_A(\mathbf{r}),\rho(\mathbf{r})] = F_{ex}[\rho_{Ad},\rho_d] + \int d\mathbf{r}\left.\frac{\delta F_{ex}}{\delta\rho(\mathbf{r})}\right|_{\rho_{Ad},\rho_d}[\rho(\mathbf{r}) - \rho_d] + \int d\mathbf{r}\left.\frac{\delta F_{ex}}{\delta\rho_A(\mathbf{r})}\right|_{\rho_{Ad},\rho_d}[\rho_A(\mathbf{r}) - \rho_{Ad}] + \frac{1}{2}\int d\mathbf{r}'\, d\mathbf{r}\left.\frac{\delta^2 F_{ex}}{\delta\rho(\mathbf{r})\delta\rho(\mathbf{r}')}\right|_{\rho_{Ad},\rho_d}[\rho(\mathbf{r}) - \rho_d][\rho(\mathbf{r}') - \rho_d] + \int d\mathbf{r}'\, d\mathbf{r}\left.\frac{\delta^2 F_{ex}}{\delta\rho(\mathbf{r})\delta\rho_A(\mathbf{r}')}\right|_{\rho_{Ad},\rho_d}[\rho(\mathbf{r}) - \rho_d][\rho_A(\mathbf{r}') - \rho_{Ad}] + \frac{1}{2}\int d\mathbf{r}'\, d\mathbf{r}\left.\frac{\delta^2 F_{ex}}{\delta\rho_A(\mathbf{r})\delta\rho_A(\mathbf{r}')}\right|_{\rho_{Ad},\rho_d}[\rho_A(\mathbf{r}') - \rho_{Ad}][\rho_A(\mathbf{r}) - \rho_{Ad}] + \ldots \qquad (5)$$

The Helmholtz free energy of the diblock copolymer system studied here is obtained directly from the coarse-grained microscopic Hamiltonian, which is taken to be

the generalized Edwards Hamiltonian

$$\beta H = \beta\sum_{\alpha=1}^{n}\sum_{i=1}^{N}\frac{\mathbf{p}_{\alpha,i}^{\,2}}{2m} + \frac{3}{2l^2}\sum_{\alpha=1}^{n}\sum_{i=1}^{N-1}(\mathbf{R}_{\alpha,i+1}-\mathbf{R}_{\alpha,i})^2 + \frac{1}{2}\sum_{\alpha,\beta=1}^{n}\sum_{i,j=1}^{N}v(\mathbf{R}_{\alpha,i}-\mathbf{R}_{\beta,j}) \quad (6)$$

where all segments are assumed to have the same mass m and the Kuhn length l is the same for both blocks. $\mathbf{R}_{\alpha,i}$ and $\mathbf{p}_{\alpha,i}$ are, respectively, the position and momentum of the ith segment on chain α. $v(\mathbf{R}_{\alpha,i}-\mathbf{R}_{\beta,j})$ is the short-ranged pairwise interaction and is different for different types of segment pairs such as A–A, A–B, and B–B. β^{-1} is the Boltzmann constant times the temperature T.

The explicit result for $F_{ex}[\rho(\mathbf{r}),\rho_A(\mathbf{r})]$ used in our work was determined by Leibler[28] using the random-phase approximation and we merely quote the result below. The ideal contribution $F_{id}[\rho(\mathbf{r}),\rho_A(\mathbf{r})]$ can readily be obtained by considering the canonical ensemble and taking the interaction term $v(\mathbf{R}_{\alpha,i}-\mathbf{R}_{\beta,j})$ in the Hamiltonian above to be zero. It is given by

$$F_{id} = -\frac{1}{\beta}\ln Z_{id} \quad (7)$$

where

$$Z_{id} = \frac{1}{n!h^{3nN}}\left[\int\prod_{i=1}^{N}d\mathbf{p}_i\prod_{j=1}^{N}d\mathbf{R}_j \times \exp\left(-\frac{\beta}{2m}\sum_{i=1}^{N}\mathbf{p}_i^{\,2} - \frac{3}{2l^2}\sum_{j=1}^{N-1}(\mathbf{R}_{j+1}-\mathbf{R}_j)^2\right)\right]^n$$

$$Z_{id} = \frac{V^n}{n!}\left(\frac{2\pi l^2}{3}\right)^{\frac{3n}{2}(N-1)}\lambda_T^{-3Nn} \quad (8)$$

where

$$\lambda_T = (\beta h^2/2\pi m)^{1/2}$$

with h being the Planck constant. Defining $\rho = Nn/V$ as the total segment density and substituting eq 8 into eq 7, we get

$$F_{id}(\rho) = \frac{V}{\beta N}\rho(\ln\rho - \theta_N) \quad (9)$$

where

$$\theta_N = 1 + \ln N + \frac{3}{2}(N-1)\ln\left(\frac{2\pi l^2}{3}\right) - 3N\ln\lambda_T$$

If ρ is not a constant as assumed here but a spatially varying quantity $\rho(\mathbf{r})$, F_{id} becomes

$$F_{id}[\rho(\mathbf{r})] = \frac{1}{\beta N}\int d\mathbf{r}\,\rho(\mathbf{r})\,[\ln\rho(\mathbf{r}) - \theta_N] \quad (10)$$

It is to be noted that this result is the direct generalization of F_{id} for monatomic systems, now accounting for the polymer chain connectivity. Therefore, F_{id} for monatomic systems can be recovered by taking the limit $N = 1$ in eq 10. Also, different choices for F_{id} of polymers, other than the one used here, have been made previously by other investigators.[39,40]

By combining eqs 1, 3, 5, and 10 we obtain the expression for the difference in grand potential between an ordered state with densities $\rho(\mathbf{r})$ and $\rho_A(\mathbf{r})$ and a disordered state with densities ρ_d and ρ_{Ad} to be

$$\Omega[\rho_A(\mathbf{r}),\rho(\mathbf{r})] - \Omega[\rho_{Ad},\rho_d] = \frac{1}{\beta N}\int d\mathbf{r}\,\rho(\mathbf{r})\ln\frac{\rho(\mathbf{r})}{\rho_d} - \frac{1}{\beta N}\int d\mathbf{r}\,[\rho(\mathbf{r})-\rho_d] + \frac{1}{2}\int d\mathbf{r}'\,d\mathbf{r}\frac{\delta^2F_{ex}}{\delta\rho(\mathbf{r})\delta\rho(\mathbf{r}')}\bigg|_{\rho_{Ad},\rho_d}[\rho(\mathbf{r})-\rho_d][\rho(\mathbf{r}')-\rho_d] + \int d\mathbf{r}'\,d\mathbf{r}\frac{\delta^2F_{ex}}{\delta\rho(\mathbf{r})\delta\rho_A(\mathbf{r}')}\bigg|_{\rho_{Ad},\rho_d}[\rho(\mathbf{r})-\rho_d][\rho_A(\mathbf{r}')-\rho_{Ad}] + \frac{1}{2}\int d\mathbf{r}'\,d\mathbf{r}\frac{\delta^2F_{ex}}{\delta\rho_A(\mathbf{r})\delta\rho_A(\mathbf{r}')}\bigg|_{\rho_{Ad},\rho_d}[\rho_A(\mathbf{r}')-\rho_{Ad}][\rho_A(\mathbf{r})-\rho_{Ad}] + \ldots \quad (11)$$

In obtaining the expression for F_{ex} by use of the random-phase approximation, Leibler[28] employed the incompressibility constraint

$$\rho_A(\mathbf{r}) + \rho_B(\mathbf{r}) = \rho$$

where ρ is independent of $\mathbf{r}$. Although this constraint need not be employed in the present calculational scheme, we will however adhere to this constraint in the present paper. Therefore, F_{ex} remains a functional of $\rho_A(\mathbf{r})$ but now is only a function of ρ. The explicit form of F_{ex} obtained by Leibler is

$$F_{ex}[\rho_A(\mathbf{r}),\rho] = \frac{1}{2\beta\rho V}\sum_{\mathbf{k}}\rho_A(\mathbf{k})\rho_A(-\mathbf{k})\left[\frac{F(x,f)}{N} - 2\chi\right] + \frac{1}{6\beta\rho^2V^2}\sum_{\mathbf{k}}\sum_{\mathbf{k}'}\Gamma_3(\mathbf{k},\mathbf{k}',-\mathbf{k}-\mathbf{k}')\rho_A(\mathbf{k})\rho_A(\mathbf{k}')\rho_A(-\mathbf{k}-\mathbf{k}') + \frac{1}{24\beta\rho^3V^3}\sum_{\mathbf{k}_1}\sum_{\mathbf{k}_2}\sum_{\mathbf{k}_3}\Gamma_4(\mathbf{k}_1,\mathbf{k}_2,\mathbf{k}_3,-\mathbf{k}_1-\mathbf{k}_2-\mathbf{k}_3)\rho_A(\mathbf{k}_1)\times\rho_A(\mathbf{k}_2)\rho_A(\mathbf{k}_3)\rho_A(-\mathbf{k}_1-\mathbf{k}_2-\mathbf{k}_3) + \ldots \quad (12)$$

where $\rho_A(\mathbf{k})$ is the Fourier transform of $\rho_A(\mathbf{r})$

$$\rho_A(\mathbf{k}) = \int d\mathbf{r}\,e^{i\mathbf{k}\cdot\mathbf{r}}\rho_A(\mathbf{r}) \quad (13)$$

and the sums over the wave vectors $\mathbf{k}$ exclude $\mathbf{k} = 0$. χ is the Flory interaction parameter for the A and B segments comprising the diblock copolymer. $F(x,f)$ is given by

$$F(x,f) = \frac{g(1,x)}{\left\{g(f,x)g(1-f,x) - \frac{1}{4}[g(1,x)-g(f,x)-g(1-f,x)]^2\right\}}$$

$$g(f,x) = (2/x^2)[e^{-fx} - 1 + fx] \quad (14)$$

where

$$x = k^2R_g^{\,2} \text{ with } R_g^{\,2} = Nl^2/6$$

As was employed in the past by other workers on diblock copolymers, we will make the local approximation for $\Gamma_3(\mathbf{k}_1,\mathbf{k}_2,\mathbf{k}_3)$ and $\Gamma_4(\mathbf{k}_1,\mathbf{k}_2,\mathbf{k}_3,\mathbf{k}_4)$, which consists of taking $\Gamma_3(\mathbf{k}_1,\mathbf{k}_2,\mathbf{k}_3) = \Gamma_3(1)$ and $\Gamma_4(\mathbf{k}_1,\mathbf{k}_2,\mathbf{k}_3,\mathbf{k}_4) = \Gamma_4(0,0)$, where $\Gamma_3(1)$ and $\Gamma_4(0,0)$ are coefficients defined by Leibler.[28]

To accomplish the minimization condition of eq 2, we follow the customary procedure in density functional theory and express $\rho_A(\mathbf{r})$ in a Fourier series specific to the particular morphology being studied

$$\rho_A(\mathbf{r}) = \rho f_A(\mathbf{r}) = \rho f + \sum_{\mathbf{k}_n}{}'\rho[a_n\cos(\mathbf{k}_n\cdot\mathbf{r}) + b_n\sin(\mathbf{k}_n\cdot\mathbf{r})] \quad (15)$$

where $f_A(\mathbf{r}) = \rho_A(\mathbf{r})/\rho$ is the reduced density profile and $\{\mathbf{k}_n\}$ are the reciprocal lattice vectors of the morphology being studied. The prime on the summation indicates

that the sum is over $\mathbf{k}_n$ but not $-\mathbf{k}_n$ and excludes $\mathbf{k}_n = 0$. The coefficients $\{a_n\}$ and $\{b_n\}$ are the order parameters of the theory and are determined by the minimization procedure. In general, the phase with the lowest grand potential is taken as the stable phase.

Combining eqs 11, 12, and 15, the dimensionless grand potential difference per chain between an ordered state with densities ρ and $\rho_A(\mathbf{r})$ and a disordered phase with densities ρ_d and ρ_{Ad} is

$$\frac{\beta N(\Omega_0 - \Omega_d)}{\rho_d V} = (1+\eta)\ln(1+\eta) - \eta - f^3\eta^3 \times \left[\frac{N\Gamma_3(1)}{6}(2\eta - 1) - \frac{N\Gamma_4(0,0)}{24}f\eta\right] - \frac{1}{4}(1+\eta)^2(1-\eta+\eta^2)\sum_{\mathbf{k}_n}'(a_n^2 + b_n^2)[2\chi N - F(x,f)] - \eta(1+\eta)^2 f\sum_{\mathbf{k}_n}'(a_n^2 + b_n^2)\left[\frac{N\Gamma_3(1)}{4}(2\eta - 1) - \frac{N\Gamma_4(0,0)}{8}\eta f\right] - \frac{1}{8}(1+\eta)^3[N\Gamma_3(1)(2\eta - 1) - N\Gamma_4(0,0)\eta f] \times \sum_{\mathbf{k}_n}'\sum_{\mathbf{k}_m}'(a_n a_m a_{n+m} + 2a_n b_m b_{n+m} - b_n b_m a_{n+m}) + \frac{N\Gamma_4(0,0)}{192}(1+\eta)^4\sum_{\mathbf{k}_n}'\sum_{\mathbf{k}_m}'\sum_{\mathbf{k}_l}'(4a_n a_m a_l a_{n+m+l} + 3a_n a_m a_l a_{n+l-m} - 4b_n b_m b_l b_{n+m+l} + 3b_n b_m b_l b_{m+l-n} - 12b_n b_m a_l a_{n+m+l} + 12a_n a_m b_l b_{n+m+l} + 12a_n a_m b_l b_{m+l-n} - 6a_n a_m b_l b_{n+m-l}) + \ldots \quad (16)$$

Here $\eta = (\rho - \rho_d)/\rho_d$ is the reduced density difference between an ordered state with total segment density ρ and a disordered state with the same chemical potential as the ordered state and density ρ_d.

In this paper we are solely interested in the ordering of diblock copolymers from the disordered state to the lamellar morphology. To simplify the minimization procedure, we have parameterized the reduced density profile $f_A(\mathbf{r})$ for the lamellar morphology as

$$f_A(z) = \frac{\rho_A(z)}{\rho_d} = f + \sum_{n=1}^{\infty}\frac{1}{\pi n}\sin(2\pi n f)\cos\left(\frac{2\pi n z}{D}\right)e^{-2\pi^2 n^2\left(\frac{\sigma_0}{D}\right)^2} \times \left(\frac{\sigma_0}{D}\right)^2 + \sum_{n=1}^{\infty}\frac{1}{\pi n}[1 - \cos(2\pi n f)]\sin\left(\frac{2\pi n z}{D}\right)e^{-2\pi^2 n^2\left(\frac{\sigma_0}{D}\right)^2} \quad (17)$$

where D is the domain spacing or lamellar repeat distance and σ_0 characterizes the sharpness of the interface between A-rich and B-rich domains. z is the position variable perpendicular to the A–B lamellar domains. A sharp interface corresponds to $\sigma_0 \ll 1$ and as σ_0 increases the interface becomes increasingly diffuse.

By comparing eqs 15 and 17 we identify

$$a_n = \frac{1}{\pi n}\sin(2\pi n f)e^{-2\pi^2 n^2\left(\frac{\sigma_0}{D}\right)^2}$$

$$b_n = \frac{1}{\pi n}[1 - \cos(2\pi f n)]e^{-2\pi^2 n^2\left(\frac{\sigma_0}{D}\right)^2}$$

with

$$x = k^2 R_g^2 = 4\pi^2 n^2\left(\frac{R_g}{D}\right)^2 \text{ and } R_g^2 = Nl^2/6$$

Therefore the present parametrization of the density profile has enabled us to write the order parameters $\{a_n\}$ and $\{b_n\}$ for the lamellar morphology using only two variational parameters σ_0 and D. Notice that these parameters appear as σ_0/D and R_g/D. Thus D is expressed in units of R_g, which is proportional to $N^{0.5}$.

In summary, there are three variational parameters σ_0/D, R_g/D, and η and four experimental variables R_g, χN, f, and ρ_d. As we emphasized above, we consider here only the ordering to the lamellar morphology. For a given choice of the experimental variables, $\Omega_0 - \Omega_d$ of eq 16 needs to be minimized with respect to σ_0/D, R_g/D, and η. Upon minimization of Ω_0, the equilibrium density ρ_0 of the ordered phase and the characteristics of the reduced density profile $f_A(z)$ (i.e., σ_0/D and R_g/D) are obtained. The phase with the lowest grand potential Ω is the thermodynamically stable phase.

If $\Omega_0 - \Omega_d$ at the calculated minimum is positive, the ordered state is less stable than the disordered state. When the minimum of $\Omega_0 - \Omega_d$ is negative, the ordered state characterized by reduced density $f_A(z)$ is the stable phase. The order–disorder transition occurs when the minimum of $\Omega_0 - \Omega_d$ is zero, since we have already imposed the equality of T, V, and μ for the two phases in the above derivation.

III. Results and Discussion

We now present the results of the calculations outlined above for the case of symmetric diblock copolymers, $f = {}^1/_2$, ordering to the lamellar morphology. To begin with we assume that there is no volume change accompanying the transition, i.e., $\eta = 0$. Also the infinite Fourier expansion for the reduced density, $f_A(z)$, was truncated at a finite number of terms determined by the requirement that the sums in eq 15 have fully converged. The following results are obtained by keeping up to 300 terms in the Fourier expansion for $f_A(z)$.

The order–disorder transition takes place at $\chi N = 10.495$ in agreement with the original prediction of Leibler.[28] By taking $\eta = 0$, the transition turns out to be second order again in agreement with Leibler. Preliminary results based on the calculation where η is a free variational parameter indicate that the transition becomes very weakly first order and this, along with the full phase diagram with all possible morphologies for different values of f, will be the subject of a future paper. We now restrict ourselves to the features of the reduced density profile $f_A(z)$ for the lamellar morphology as χN is varied.

The equilibrium values of the domain spacing D and σ_0, the parameter characterizing the sharpness of the interface, are given in Table I and plotted in Figures 1 and 2. The table also contains the minimum values of $\Omega_0 - \Omega_d$ for different χN values. Although the figures contain the same information as the table, the raw data are provided for the convenience of the reader. In Figure 1, $\ln(D/R_g)$ is plotted against $\ln(\chi N)$. As pointed out earlier the order–disorder transition takes place at $\chi N = 10.495$. It is clear from Figure 1 that there are three distinct regimes for the molecular weight dependence of the domain spacing D.

For values of χN in the range 10.495–12.5, D/R_g (=3.23) is independent of χN. Consequently, in this regime D is proportional to R_g and therefore the domain spacing is proportional to $N^{0.5}$. In addition, D is independent of χ for $10.495 \le \chi N \le 12.5$. We identify this regime to be the weak segregation regime of Leibler[28] and have clearly determined the range of the weak segregation limit in χN. In the weak segregation limit, the A segment density is considered to vary in a sinusoidal fashion. Also, the junction points between the A-type chains and B-type chains are distributed approximately at random in space. A typical reduced density profile $f_A(z) = \rho_A(z)/\rho$ in the

Table I
Equilibrium Values for the Variational Parameters D/R_g and σ_0/D and $\beta N/\rho V$ ($\Omega_0 - \Omega_d$) Calculated by Using Density Functional Theory for the Lamellar Morphology with $f = 0.5$ and $\eta = 0$

χN	D/R_g	σ_0/D	$\beta N\Delta\Omega/\rho V$
10.495	3.231	0.549 69	-0.3875×10^{-9}
10.503	3.231	0.398 73	-0.1547×10^{-5}
11.000	3.231	0.233 24	-0.2368×10^{-2}
11.500	3.231	0.192 05	−0.02368
12.000	3.231	0.162 28	−0.05335
12.500	3.231	0.136 72	−0.09552
13.000	3.241	0.117 63	−0.1495
14.000	3.273	0.097 831	−0.2794
15.000	3.306	0.086 908	−0.4256
16.000	3.350	0.078 087	−0.5822
17.000	3.390	0.072 802	−0.7467
18.000	3.431	0.067 703	−0.9175
19.000	3.472	0.063 384	−1.0936
20.000	3.509	0.059 740	−1.274
21.000	3.546	0.056 556	−1.459
23.000	3.623	0.051 218	−1.837
27.000	3.752	0.043 598	−2.625
30.000	3.846	0.039 396	−3.234
35.000	3.976	0.034 275	−4.277
40.000	4.090	0.030 544	−5.345
45.000	4.184	0.027 729	−6.431
50.000	4.283	0.025 409	−7.531
55.000	4.357	0.023 594	−8.643
65.000	4.505	0.020 714	−10.89
75.000	4.630	0.018 585	−13.17
95.000	4.843	0.015 592	−17.79
105.00	4.938	0.014 482	−20.12
125.00	5.102	0.012 766	−24.81
145.00	5.236	0.011 499	−29.54
175.00	5.420	0.010 064	−36.68
195.00	5.525	0.93314×10^{-2}	−41.47
225.00	5.666	0.84490×10^{-2}	−48.659
255.00	5.797	0.77412×10^{-2}	−55.88
285.00	5.917	0.71625×10^{-2}	−63.13
335.00	6.079	0.64173×10^{-2}	−75.25

weak segregation regime is plotted in Figure 3 against z/D for $\chi N = 11.00$. For this value of χN, $D/R_g = 3.23$ and $\sigma_0/D = 0.233\,24$. Notice the approximately sinusoidal nature of the density profile. It is also obvious from Figure 2 that for $10.495 \leq \chi N \leq 12.5$, a simple power law for the χN dependence of interface parameter σ_0 cannot be established. In fact, σ_0 appears to diverge as χN approaches the critical value $(\chi N)_c = 10.495$.

Far away from the order–disorder transition, characterized by $\chi N > 105$, we observe from Figure 1 the scaling behavior

$$D/R_g \propto (\chi N)^{0.17\pm0.01} \tag{18}$$

For $\chi N > 335$ the asymptotic result $D/R_g \propto (\chi N)^{0.17}$ is achieved. Therefore

$$D \propto N^{0.67}\chi^{0.17} \tag{18'}$$

The N exponent is in agreement with the earlier prediction of $^2/_3$ by the theories for the strong segregation limit. Thus we identify the regime $\chi N > 100$ as the strong segregation regime. In this regime, the reduced density profile $f_A(z)$ for a typical value of $\chi N = 195$ is shown in Figure 4. The values of the two variational parameters R_g/D and σ_0/D are 0.1810 and 0.93314×10^{-2}, respectively. The strong segregation regime is characterized by well-defined A and B domains separated by a very narrow interface. In the strong segregation limit, σ_0, the parameter that characterizes the breadth of the interface, varies with χN according to the power law (see Figure 2)

$$\sigma_0/D \propto (\chi N)^{-0.69\pm0.01} \tag{19}$$

Again for $\chi N > 335$ the asymptotic result $\sigma_0/D \propto (\chi N)^{-0.67}$ is obtained, so that

$$\sigma_0 \propto \chi^{-0.50\pm0.02} \tag{20}$$

where the result of eq 18 was used. Since σ_0 is proportional to the interfacial thickness, we find that the interface thickness is independent of molecular weight and varies as $\chi^{-0.5}$ in the strong segregation regime. This too is in agreement with previous theories of the strong segregation regime.

Between the weak and strong segregation limits we are able to clearly identify from Figure 1 an intermediate regime with features distinctly different from those of weak and strong segregation regimes. In this crossover regime, we find the result

$$D \propto N^{0.72}\chi^{0.22}$$

for values of χN in the range $17 \leq \chi N \leq 80$. Note that the N exponent of D is higher in the intermediate regime than in the strong segregation limit. The density profile for a typical value of $\chi N = 35$ in the intermediate regime

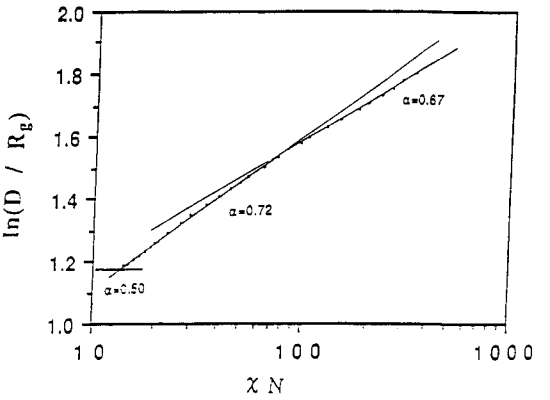

Figure 1. Plot of $\ln(D/R_g)$ vs $\ln(\chi N)$ for the lamellar morphology with $f = 0.5$ and $\eta = 0$.

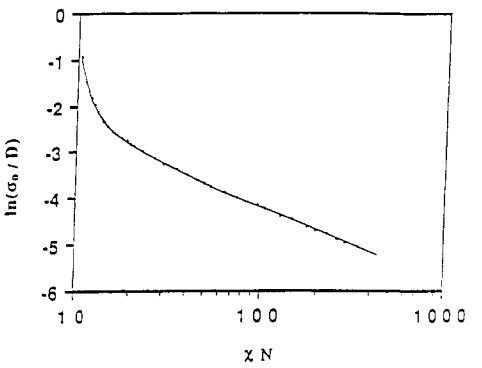

Figure 2. Plot of $\ln(\sigma_0/D)$ vs $\ln(\chi N)$ for the lamellar morphology with $f = 0.5$ and $\eta = 0$.

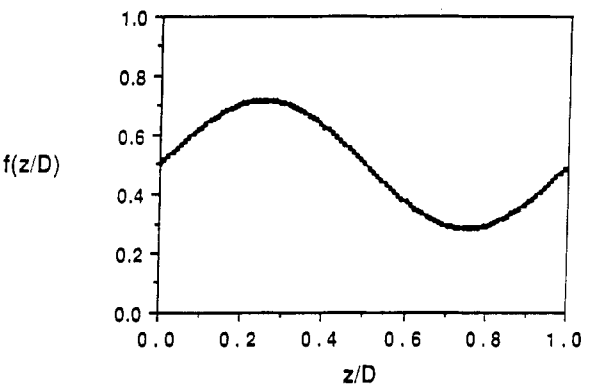

Figure 3. Plot of the reduced density $f_A(z/D)$ vs z/D for $\chi N = 11$ ($D/R_g = 3.23$ and $\sigma_0/D = 0.233$).

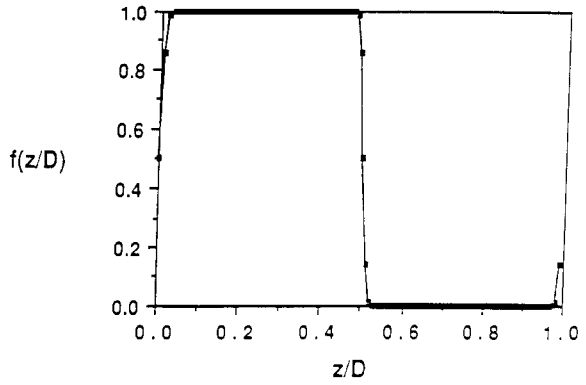

Figure 4. Plot of the reduced density $f_A(z/D)$ vs z/D for χN = 195 (D/R_g = 5.52 and σ_0/D = 0.00933).

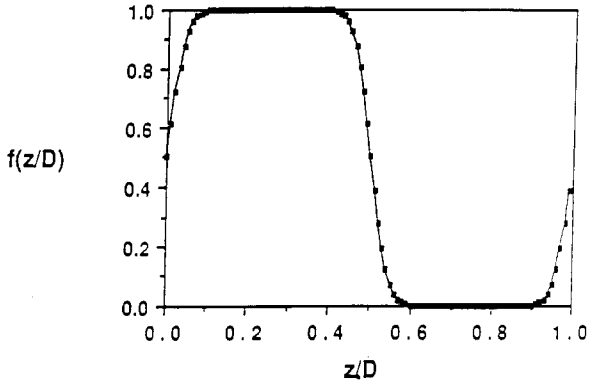

Figure 5. Plot of the reduced density $f_A(z/D)$ vs z/D for χN = 35 (D/R_g = 3.98 and σ_0/D = 0.0343).

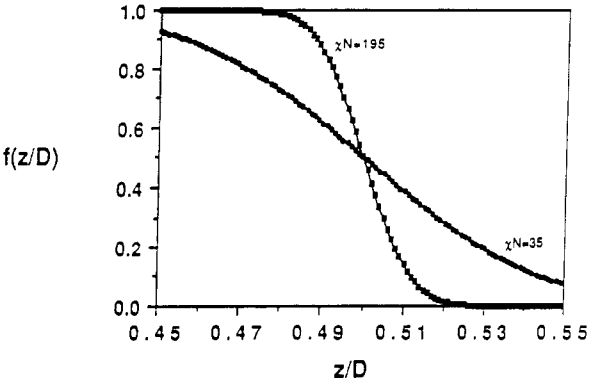

Figure 6. Plot of the reduced density $f_A(z/D)$ vs z/D in the interfacial region for (●) χN = 35 (D/R_g = 3.98 and σ_0/D = 0.0343) and (■) χN = 195 (D/R_g = 5.52 and σ_0/D = 0.00933).

is presented in Figure 5 where R_g/D = 0.2515 and σ_0/D = 0.0343. Although the interface is narrow, it is not very sharp in comparison with a typical density profile in the strong segregation regime. The details of the interfacial region for χN = 35 and 195 are compared in Figure 6. The N scaling exponent of D with a power greater than $^2/_3$ is attributed to the coarsening of the density profile as χN is increased from the weak segregation limit. To accomplish this, the junction points between the diblock chains must move into the interfacial region. In addition, because the interfacial region in the intermediate regime is spread over a wider range of space than with the strong segregation limit (see Figure 6), the junction points are not completely localized in the intermediate regime. These effects, coupled with the stretching of the chains that arises from the requirement that the total segment density ρ be uniform in space, give rise to the N exponent of D being greater than that for the strong segregation limit. Last, it is clear from Figure 2 that a single power law cannot be used to accurately describe the χN dependence of the

Table II
Equilibrium Values for the Parameters D/R_g and σ_0/D Calculated by Using Density Functional Theory for Block Copolymer Compositions f and χN Values Considered in Reference 18

f	χN	D/R_g	σ_0/D
0.50	10.5	3.231	0.549 69
0.496	35.0	3.976	0.034 294
0.473	42.0	4.124	0.029 642
0.534	105.0	4.950	0.014 437

interfacial parameter σ_0/D in the intermediate regime. However, we find that σ_0 is only weakly dependent on N in the intermediate regime.

The key result of the density functional theory presented here is the occurrence of a well-defined intermediate regime intervening between the weak and strong segregation limits. The boundaries of this new regime have been identified to be $15 \leq \chi N \leq 90$. The exponent for the N dependence of the domain spacing D in this new regime is 0.72. The value of this exponent may change when the volume change accompanying the ordering process is taken into account.

We now make a comparison between the results of the present density functional theory and some recent experimental investigations. The prediction that the N scaling exponent of D is higher than that of the strong segregation limit as χN is increased from the weak segregation limit is in qualitative agreement with the value of 0.8 for this exponent reported recently by Almdal et al.[19] and in the past by Hadziioannou and Skoulios.[10] However, these investigations have not observed the crossover from the intermediate regime to the strong segregation regime. It remains unclear at present whether the observed result in these experiments is truely an intermediate behavior or an asymptotic limit with an entirely different mechanism dominating the ordering process. Assuming that the experimentally observed result, $D \propto N^{0.8}$, actually corresponds to the intermediate regime, the difference between 0.8 and 0.72 is not profound as this exponent is nonuniversal and depends on compressibility, chain stiffness, etc.

Finally, we comment on the puzzling conclusion of Anastasiadis et al.,[18] who observed $D \propto N^{0.65}$ apparently in agreement with strong segregation theories even though their lowest molecular weight sample (used in obtaining the strong segregation exponent) was shown to be in the weak segregation regime at the temperature of the study. This conclusion is merely a reflection of a lack of a full set of data. They have considered only four samples with χN = 10.5, 35, 42, and 105 with f = 0.5, 0.496, 0.473, and 0.534, respectively. In these experiments, f is the fraction of styrene segments in a polystyrene–poly(methyl methacrylate) diblock copolymer. In addition, all four samples considered by Anastasiadis et al. were of the lamellar morphology. When compared with Figure 1, it is clear that, with their lowest molecular weight sample (χN = 10.5 and f = 0.473) in the weak segregation regime, the two samples corresponding to χN = 35 (f = 0.496) and χN = 42 (f = 0.473) lie in the intermediate regime. Their highest molecular weight sample χN = 105 (f = 0.534) is then at the leading edge of the strong segregation regime. As a consequence, an apparent exponent between 0.5, 0.72, and 0.67 for the N scaling of the domain spacing D could be observed. To explore this issue further, we have performed the calculations using the density functional theory developed here for the particular values of f and χN considered in the experiments of Anastasiadis et al. The results are shown in Table II. We obtain an apparent exponent of 0.68, that is $D \propto N^{0.68}$, in remarkable agreement

with their reported value of 0.65. Of course, this is only an apparent result between the weak segregation limit, intermediate regime, and strong segregation limit and definitely is not due to the occurrence of the strong segregation limit.

Finally, we conclude by making a few technical remarks. The particular parametrization of the density profile, eq 14, makes the infinite sum rapidly convergent. Furthermore, we find that in our current work the fourth-order term in the expansion for $\beta N\delta\Omega/\rho V$ makes less than a 1% contribution to the total value of $\beta N\delta\Omega/\rho V$ in the strong segregation limit. The convergence behavior observed here with density functional theory should be contrasted with other theories for the strong segregation limit based on expansions in the composition difference order parameter.[25] Suffice to say, density functional theory includes all wave vectors in the expression for the grand potential of the ordered phase. All of the theories of weak segregation limit employ the approximation of the domination by one wave vector corresponding to the maximum of the structure factor. We find from our calculations that this is a good approximation only for $\chi N \leq 11.0$. So the phase diagram calculated on the basis of the current weak segregation theories should only be reliable very close to $(\chi N)_c$.

Acknowledgment. We thank Dr. Scott M. Cohen for useful discussions. This work was supported by the National Science Foundation Grant DMR9008192 and the Materials Research Laboratory at the University of Massachusetts.

References and Notes

(1) Bates, F. S.; Fredrickson, G. H. *Annu. Rev. Phys. Chem.* **1990**, *41*, 1990.
(2) Aggarwal, S. L., Ed. *Block Copolymers*; Plenum: New York, 1970.
(3) Hashimoto, T.; Nagatoshi, K.; Todo, A.; Hasegawa, H.; Kawai, H. *Macromolecules* **1974**, *7*, 364.
(4) Hashimoto, T.; Todo, A.; Itoi, H.; Kawai, H. *Macromolecules* **1977**, *10*, 377.
(5) Todo, A.; Uno, H.; Niyoshi, K.; Hashimoto, T.; Kawai, H. *Polym. Eng. Sci.* **1977**, *17*, 527.
(6) Hashimoto, T.; Shibayama, M.; Kawai, H. *Macromolecules* **1980**, *3*, 1237.
(7) Hashimoto, T.; Fujimura, M.; Kawai, H. *Macromolecules* **1980**, *13*, 1660.
(8) Fujimura, M.; Hashimoto, H.; Kurahashi, K.; Hashimoto, T.; Kawai, H. *Macromolecules* **1981**, *14*, 1196.
(9) Bates, F. S.; Berney, C. V.; Cohen, R. E. *Macromolecules* **1983**, *16*, 1101.
(10) Hadziioannou, G.; Skoulios, A. *Macromolecules* **1982**, *15*, 258.
(11) Richards, R. W.; Thomson, J. L. *Macromolecules* **1983**, *16*, 982.
(12) Bates, F. S.; Cohen, R. E.; Berney, C. V. *Macromolecules* **1982**, *15*, 584.
(13) Alward, D. B.; Kinning, D. J.; Thomas, E. L.; Fetters, L. J. *Macromolecules* **1986**, *19*, 215.
(14) Kinning, D. J.; Alward, D. B.; Thomas, E. L.; Fetters, L. J.; Handlin, D. J. *Macromolecules* **1986**, *19*, 1288.
(15) Thomas, E. L.; Alward, D. B.; Kinning, D. J.; Handlin, D. L.; Fetters, L. J. *Macromolecules* **1986**, *19*, 2197.
(16) Herman, D. S.; Kinning, D. J.; Thomas, E. L.; Fetters, L. J. *Macromolecules* **1987**, *20*, 2940.
(17) Hasegawa, H.; Tanaka, H.; Yamasaki, K.; Hashimoto, T. *Macromolecules* **1987**, *20*, 1651.
(18) Anastasiadis, S. H.; Russell, T. P.; Satija, S. K.; Majkrzak, C. F. *J. Chem. Phys.* **1990**, *92*, 5677.
(19) Almdal, K.; Rosedale, J. H.; Bates, F. S.; Wignall, G. D.; Fredrickson, G. H. *Phys. Rev. Lett.* **1990**, *65*, 1112.
(20) Matsushita, Y.; Mori, K.; Saguchi, R.; Nakao, Y.; Noda, I.; Nagasawa, M. *Macromolecules* **1990**, *23*, 4313.
(21) Meier, D. J. *J. Polym. Sci. C* **1969**, *26*, 81.
(22) Helfand, E. *Macromolecules* **1975**, *8*, 552.
(23) Helfand, E.; Wasserman, Z. R. *Macromolecules* **1976**, *9*, 879; **1978**, *11*, 960; **1980**, *13*, 994.
(24) Semenov, A. N. *Sov. Phys.—JETP (Engl. Transl.)* **1985**, *61*, 733.
(25) Ohta, T.; Kawasaki, K. *Macromolecules* **1986**, *19*, 2621. Kawasamki, K.; Ohta, T.; Kohrogui, M. *Macromolecules* **1988**, *22*, 2972.
(26) Kawasaki, K.; Kawakatsu, T. *Macromolecules* **1990**, *23*, 4006.
(27) DiMarzio, E. A. *Macromolecules* **1988**, *21*, 2262.
(28) Leibler, L. *Macromolecules* **1980**, *13*, 1602.
(29) Fredrickson, G. H.; Helfand, E. *J. Chem. Phys.* **1987**, *87*, 6.
(30) Ramakrishnan, T. V.; Yussouff, M. *Phys. Rev. B* **1977**, *19*, 2775.
(31) Haymet, A. D. J.; Oxtoby, D. *J. Chem. Phys.* **1981**, *74*, 2559; **1986**, *84*, 1769. Haymet, A. D. J. *J. Chem. Phys.* **1983**, *78*, 4641.
(32) Singh, Y.; Stoessel, J. P.; Wolynes, P. G. *Phys. Rev. Lett.* **1985**, *54*, 1059.
(33) Smithline, S. J.; Haymet, A. D. J. *J. Chem. Phys.* **1987**, *86*, 6486.
(34) Jones, M.; Mohanty, U. *Phys. Rev. Lett.* **1987**, *58*, 230.
(35) Curtin, W. A.; Ashcroft, N. W. *Phys. Rev. A* **1985**, *32*, 2909.
(36) Tarazona, P. *Phys. Rev. A* **1985**, *31*, 2672.
(37) Baus, M.; Colot, J. L. *Mol. Phys.* **1985**, *55*, 653.
(38) Curtin, W. A. *J. Chem. Phys.* **1988**, *88*, 7050.
(39) Chandler, D.; McCoy, J. D.; Singer, S. J. *J. Chem. Phys.* **1986**, *85*, 5971; **1986**, *85*, 5977.
(40) McMullen, W. E.; Freed, K. F. *J. Chem. Phys.* **1990**, *92*, 1413.